

Microstructure and Mechanical Properties Assessments of 304 Austenitic Stainless Steel and Monel 400 Dissimilar GTAW Weldment



Mohammed Sabeeh Mohamed^{1*}, Auday Awad Abtan¹, Affaan Uthman Moosa²

¹ Training and Workshops Center, University of Technology-Iraq, Baghdad 10001, Iraq

² Applied Engineering Department Engineering Technical College, Middle Technical University, Baghdad 10071, Iraq

Corresponding Author Email: mohammed.s.mohammed@uotechnology.edu.iq

<https://doi.org/10.18280/rcma.330301>

ABSTRACT

Received: 5 February 2023

Accepted: 13 June 2023

Keywords:

migrated grain boundaries (MGBs), epitaxial growth, partial melting zone (PMZ), unmixed zone (UZ)

Monel 400 nickel alloy and AISI 304 austenitic stainless steel dissimilar fusion welding influenced in very important fields like oil, nuclear, space industries and petrochemical where high temperatures and corrosive environments are involved with weldments. Also, this dissimilar joint extremely important with environments demand high heat resistance, corrosion resistance, resistance thermal cycles consequences, creep resistance and good mechanical properties. One of the most important advantages of dissimilar welds is saving of novel and expensive materials cost. Dissimilar welding joints in this research produced with gas tungsten arc welding techniques (GTAW) and ENiCrFe-2 filler. Welding joint configuration simulated welding joint design in real working site to achieved best results and asses real welding site up. SEM/EDS analysis, optical microstructure examination, Vickers microhardness test, tensile test and V- notch impact test employed to study and understand welding microstructure details and properties and its impacts in weldment mechanical properties. Research results reveals formation of partial melting zone (PMZ), unmixed zone (UZ) and second phase in HAZ while dendritic solidification with heat flow direction, epitaxial growth, cellular epitaxial solidification and migrated grain boundaries (MGBs) observed in welding zone microstructure, this research deeply analyses formation of these phenomena, and its effects on weldments mechanical properties were discussed. This research results are very important to welding technologist and engineers to understand and prediction resultant welding zone and HAZ microstructures and understanding its impacts on required weldments design criteria when establish welding procedure.

1. INTRODUCTION

Super alloy Ni-Cu based Monel 400 having outstanding resistance to salt sea water and hot steam at elevated temperatures as well as to caustic solutions. Monel 400 Ni-based alloy offer desired characteristics like good weldability and high strength [1]. 304 austenitic stainless steel demonstrated excellent toughness and good ductility with significant elongation when subjected to tensile forces [2]. Monel 400 and AISI 304 dissimilar weldments highly required in applications must accommodate for corrosive environment with moderate strength demanded at high temperatures. These dissimilar weldments extensively used with food industry equipment, oil gasification equipment, feed water plants in boilers and petrochemical facilities [3-5].

AISI 304 and Monel 400 dissimilar fusion welding joint widely used in critical environments needed weldments requirements like corrosion resistance, high temperatures resistance, creep resistance and serviceability with designed thermal cycles and keeping its good mechanical advantages under these circumstances. According to design requirements, dissimilar welding joints will contribute to saving unique and high price costs of these materials and reducing overall production cost. Dissimilar welding generally considers as big

challenge because of mechanical, physical, and metallurgical properties difference between parent metals to be welded. Major problems expected to occur during dissimilar welding because of variation in thermal expansion coefficients and chemical composition, also these conditions will cause inconvenient dilution between filler and parents' metals, HAZ expected to suffer from liquation cracking and hot cracking, also formation of secondary phases issues. Monel 400 and AISI 304 bimetallic combinations used in application working at temperatures up to 550°C like steam generator tubing, fossil-fuel power plants, oil gasification plants and chemical processing equipment's. Monel 400 alloy welded with TIG technology investigated by Nallusamy et al. [6] research results shown excellent joint with good strength and corrosion resistance properties. Dilution of filler metal had essential effects on dissimilar welding joints, Yelamasetti and Kumar et al. [7] research revels filler wires effects on weld strength of Monel 400 and AISI 304 dissimilar weldments results clearly demonstrated the variation in weldments mechanical properties according to filler metal type. Microstructure changing resultant in residual stresses deeply effects weldments fit with design criteria, Balram et al. [8] analyses GTAW dissimilar Monel 400 and AISI 304 joint welded with ERNiCrMo-3 filler residual stresses to understanding these

effects. Monel 400 and AISI 304 bimetallic combinations used in application working at temperatures up to 550°C like steam generator tubing, fossil-fuel power plants, oil gasification plants and chemical processing equipment's. Investigations of similar metal welding by gas tungsten arc welding studied by different researchers, and welding microstructure analyses to investigated its impacts on weldments mechanical properties, Mishra et al. [9] studied confidential interface dissimilar assembly of Monel 400 and AISI 316L bimetallic joints welded with ERNiCrMo-3 filler metal and formation of migrated grain boundaries and carbides at welding zone microstructure, research result shown increasing in welding zone strength with migrated grain boundaries formation. Oil and gas gasification plants exposed welding joints to very high temperature corrosion environments, Devendranath Ramkumar et al. [10] studied dissimilar joints combinations of low carbon steel and Monel 400 and improvement of hot crack resistance in welding zone by using Nb-rich fillers. study results demonstrated the advantages of using ERNiCrMo-3 filler as Nb-rich filler wire to get important improvements in weldment properties. TIG, FRW and EBM welded joint of AISI 304 and AISI 4140 and microstructure and alteration with mechanical properties investigated by Arivazhagam et al. [11] results of research dedicated best technique to form dissimilar welded joint. Tungsten arc dissimilar welded joint shown highest impact value compared to FRW and EBM technology. Dissimilar welding joints produced by Electron Beam and Tungsten arc welding shown better ductility compared to Friction resistance joints. Shah Hosseini et al. [12] investigated fillers like Inconel 617, Inconel 82 and 310SS in stainless steel welding to Inconel alloys and austenitic phase formation in welding zone microstructure. Results showing stabilizing effects of Nb presented with 3% on austenite in austenitic microstructure matrix. Welding zone and HAZ microstructures essential to predicated weldment serviceability, Sabzevar et al. [13] calculate welding temperature distribution in welding zone and HAZ by employing multi scale model, study results shown heat distribution content of both electrodes detached liquid metal and electrical arc generated heat. Researchers also developed stochastic simulated model of austenite phase formation and growth through welding according to kinetics of the processes. Iron presence in nickel-based super alloys effects reported by Naffakh et al. [14] his results shown effect of iron presence in lower solubility of niobium in austenite matrix structure, this will not only drop-down melting point as direct effect of niobium concentration drop in structure, but also strongly involved in creation low melting austenite eutectics carbide during welding metal solidification. Migrated grain boundaries (MGBs) creation in austenitic weld metals and its prevalence in similar microstructures have been investigated in DuPont et al. [15] research paper. As reported by its research and also marked in other research papers, welding metal producing by employing filler wire with high Ni concentrations has shown a high tendency to ductility dip cracking (DDC) phenomena which usually occurs in migrated grains boundaries (MGBs), (MGBs) can be defined as crystallographic with high angle boundaries which moved away from its original locations in parent solidification structure grain boundaries when the welding metal cooling down below the weld metal solidification range temperature and/or it could happen during reheating effects which produced from multi-pass welding procedure. According to the following survey and based on research papers, and

experimental studies, employing fillers with high Mo and Nb concentrations will produce best results. Immigration of carbon in Cr-Mo joints between the welding zone and parent metal occurrence due to elemental concentration variations, especially with chromium concentration investigated by Sadek et al. [16], results concluded carbon diffusion phenomena from parent metal with lower-chromium to welding zone side, which has higher chromium and chromium carbide, and carbon diffusion zone (CDZ) formation adjacent to weld interface. Therefore, research on Monel 400 and 304 alloys dissimilar welding very important to our understanding development of essential changes in welding and HAZ microstructures and alterations of mechanical properties resulted from these changes.

2. MATERIAL AND EXPERIMENTAL WORK

Copper-Nickel alloy Monel 400, AISI 304 austenitic stainless steel provided from Iraqi Oil Ministry and ENiCrFe-2 filler metal from ESAB company chemical compositions represented in Table 1. Welding samples with 100 mm × 50 mm × 4 mm dimensions and square butt joint configurations with 2 mm root space fabricated and welded with Diversion™ 180 TIG welding technology from Miller as shown in Figure 1.

Welding samples clamped strongly in fixture with copper back plate to distract harmful welding heat from weldment and avoid distortion during welding. Welding parameters established from earlier studies and from trial and error experiments and illustrated in Table 2. After welding, weldments shaped into required dimensions using wire cut machine EDM (Electrical Discharge Machining) to investigate welding joint metallurgical and mechanical characters.

Welding zone, HAZ and parent metals microstructures metallographic examined. Metallographic test standard procedure applied to investigate weldments various zones microstructure. Weldments samples prepared using SiC emery sheets with 220 to 1000 grit size, then followed by alumina disc polishing to obtain final mirror finish of 1µm. Monel 400 nickel alloy HAZ and welding joint microstructures detected with (50 ml HCl, 10 grams of CuSO4 and 50 ml distilled water) etching reagent, while (15cc HCl, 10 cc HNO3 and 10 cc CH3COOH) etching reagent used on AISI 304 austenitic stainless steel HAZ and welding zone. ASTM E8 standard applied in tensile studies of the weldment's samples. Three samples test performed to ensure authenticity of results. 2 mm/min strain rate used for the three test samples.

Table 1. Experiment base metals and welding filler metal chemical compositions

Composition Wt.%	Monel 400	AISI 304	ENiCrFe-2
Ni	64.86	8.46	61.8
Cu	Bal.	Nil.	0.53
C	0.13	0.048	0.10
Si	0.38	0.41	0.8
Mn	1.11	1.71	3.44
Fe	2.24	Bal.	11.2
S	Nil.	0.005	0.018
P	Nil.	0.021	0.03
Cr	Nil.	18.78	Bal.
others	Nil.	Nil.	1.5(Nb),2.5(Mo)

Vickers Microhardness tester conducted to study microhardness on all three regions of weldments by keeping weld in center and test from the both sides. Microhardness test employed 500 gf load and 10 second dwell time, microhardness measurements carried out with regular 1 mm spacing and more than 20 microhardness points was taken (10 point from each side). SEM and EDS analysis employed on weldments various zones to determine the elements diffusion between the welding zone and HAZ and also to assess welding zone structure correlations with weldment mechanical properties changing.

Table 2. GTAW welding parameters

Welding Technique (GTAW (Filler))	
Voltage (volt)	10
Current (Amp)	130
Shielding Gas Flow Rate (lpm)	15
No. of Passes	2
Filler Wire Diameter (mm)	2.4

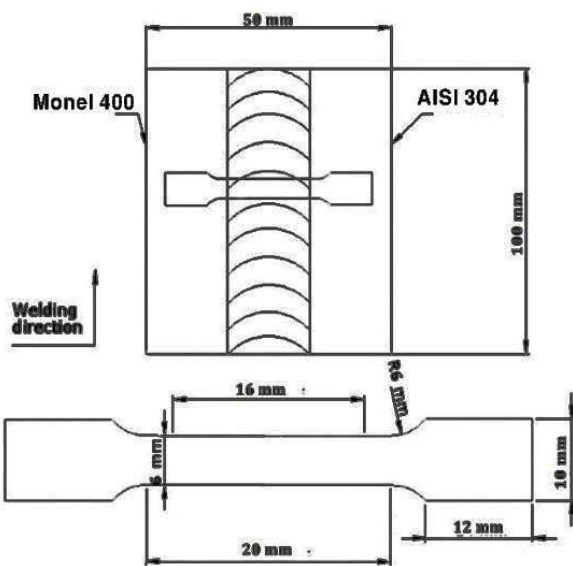


Figure 1. Monel 400 and AISI 304 weldment configuration

3. RESULTS

3.1 Monel 400 HAZ microstructural features

Optical observing of Monel 400 HAZ microstructural reveals Ni-Cu second phase formation with coarse grains size at (HAZ) microstructure as shown in Figure 2(a), (b), (c) and (d) grains size coarsening can be observed in structure due to GTA welding heat. Also, partial melting zone (PMZ) formation can be easily observed in HAZ.

3.2 AISI 304 HAZ microstructural features

AISI 304 HAZ side reveals changes in grain size, but no precipitation or sensitization evidences can be detected in microscopic microstructural examination; also, fine austenitic grains size noticed near fusion line and twinning randomly grain structure observed in little amount. Figure 3(a), (b) and (c) shown formation of welding filler metal debilitation area, unmixed zone (UZ) and fusion line. Figure 3(d) illustrated clear welding fusion line and HAZ fine grain size.

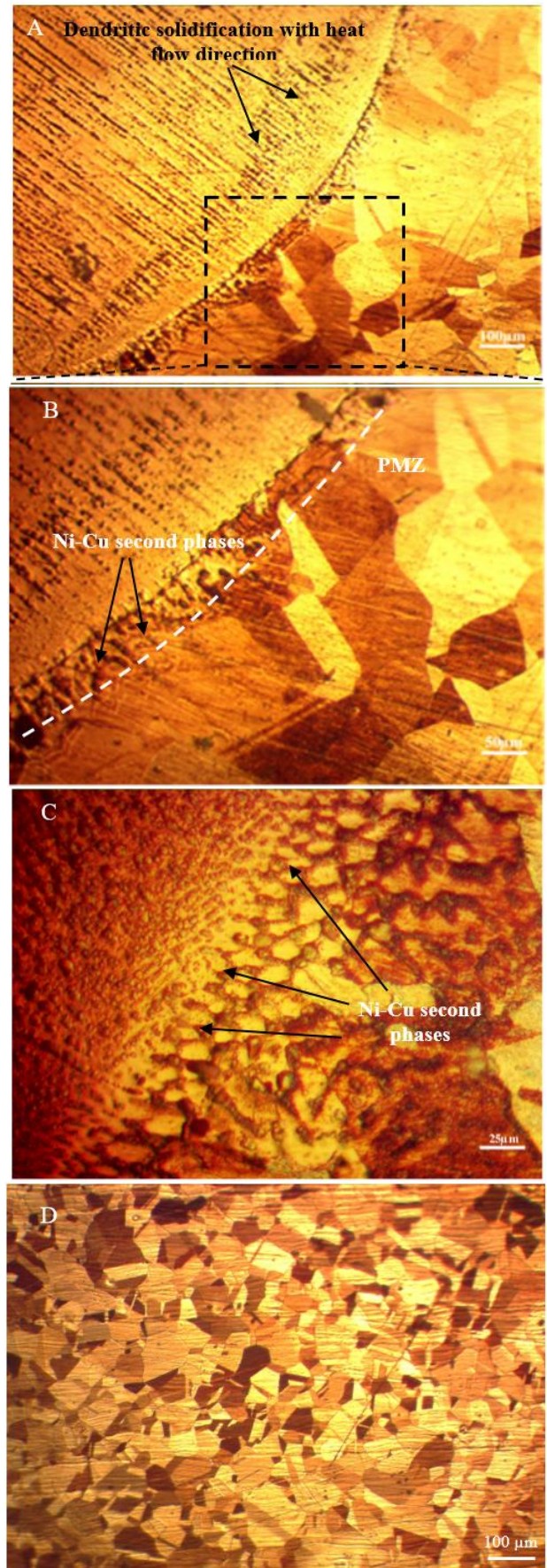


Figure 2. (a) Monel 400 HAZ and PMZ and at 200x shown the formation of welding zone structure with heat flow direction (b) PMZ and HAZ at 400x shown formation of the second phases (c) PMZ at 800x with clearly second phase formation (d) Monel 400 HAZ grain size

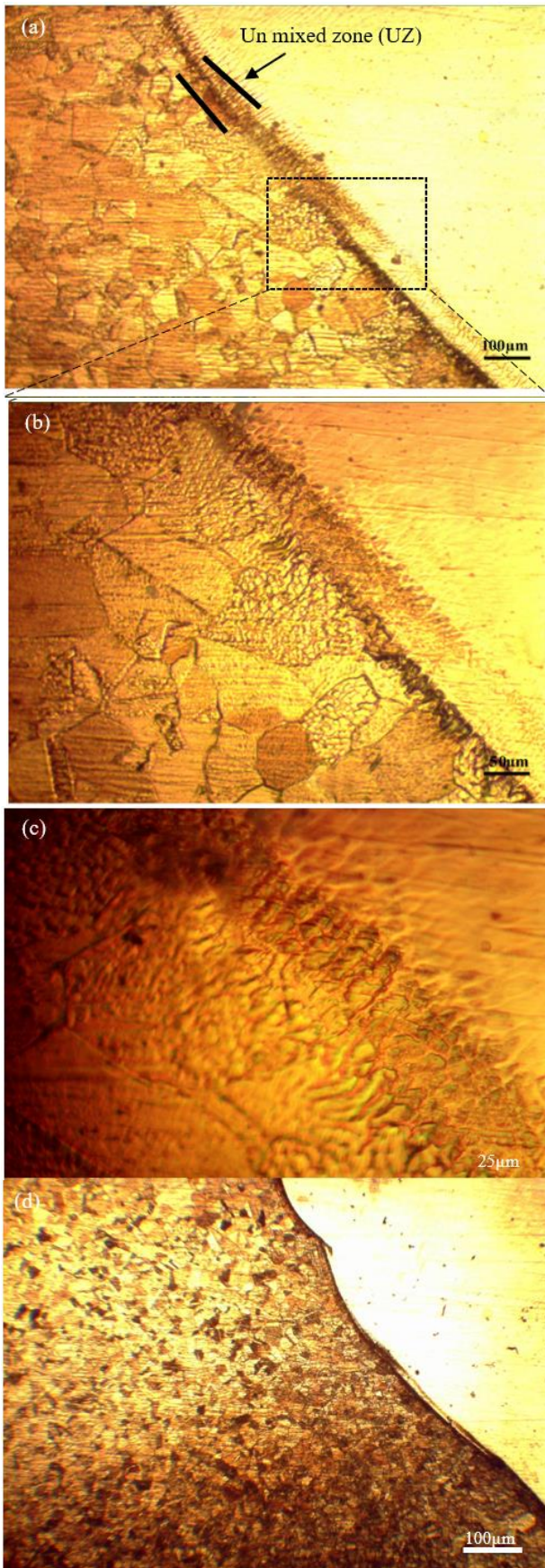


Figure 3. (a) AISI 304 weld zone just near welding fusion line of 100x shown unmixed zone formation (b) unmixed zone and fusion line at 200x and HAZ grains with no carbide precipitation (c) center of unmixed zone in fusion line at 800x (d) welding fusion line and unmixed zone with fine grain size microstructure

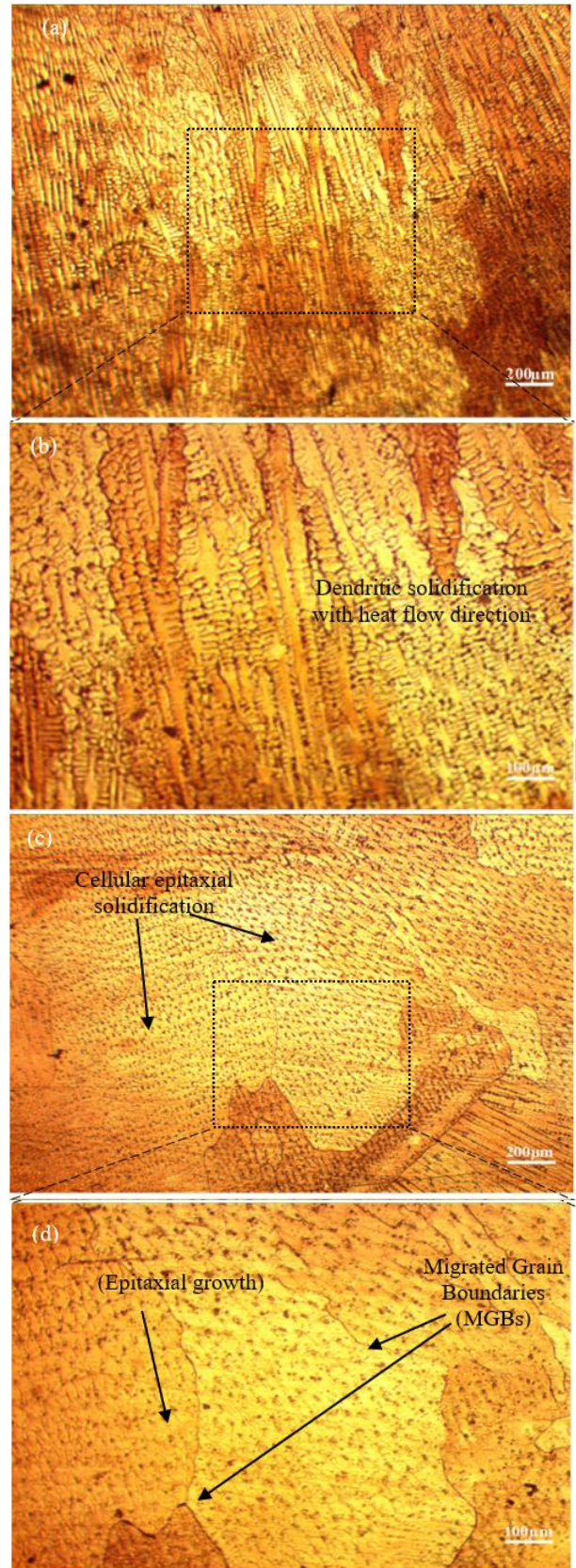


Figure 4. (a) Welding zone just near fusion line of Monel 400 at 100x shown dendritic solidification formation with heat flow direction (b) Welding zone near fusion line at 200x shown of dendritic solidification and second phases formation (c) center of welding nugget at 100x with clearly cellular epitaxial solidification formation (d) center of welding nugget at 200x with clearly cellular epitaxial solidification formation and Migrated Grains Boundaries (MGBs)

3.3 Welding zone microstructural features

Welding zone microstructure reveals extinguish interdendritic network consisting elements like Ni, Cr, Fe, Cu as shown in Figure 4(a), (b). welding zone region far from welding fusion line and welding zone center demonstrated clearly epitaxial solidification model as in Figure 4(c) and (d), migrated grain boundaries also observed clearly at welding zone. Figure 4(c) and (d) also illustrated existence of cellular solidification structure of welding zone contains some copper, secondary phases formation also can be observed; secondary phases formation makes welding metal more suspected for hot cracking defect.

4. WELDMENTS MECHANICAL PROPERTIES CHARACTERIZATION

4.1 Vickers micro hardness measurement

Monel 400 to AISI 304 dissimilar welding by using ENiCrFe-2 filler metal hardness profile clearly demonstrated maximum hardness value was recorded at welding zone, hardness value average at welding zone founded 202.2 HV while hardness average value of 192.6 HV recorded in Monel 400 HAZ and 134.6 HV for 304 austenitic stainless steel side as in Figure 5.

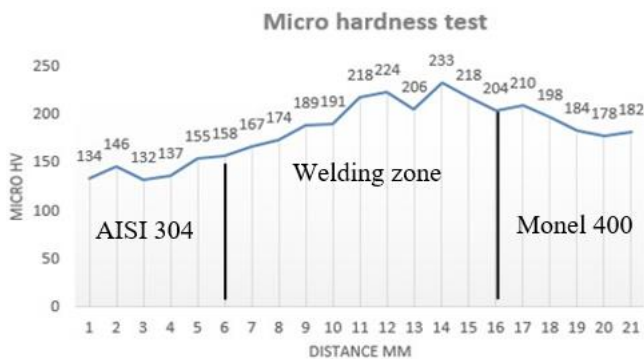


Figure 5. AISI 304 and Monel 400 dissimilar GTAW weldment micro hardness profile

4.2 Weldments tensile test

ASTM E8 standard procedure applied to prepare samples to record accuracy tensile test values of dissimilar welding joints. Three tensile tests were prepared to record the average value of the test, in all three samples; samples failure occurred at AISI 304 base metal, as shown in Figure 6. Samples before fracture suffered significant amount of plastic deformation reflecting failure in ductile style. Tensile test average properties recorded from tests include tensile strength of 503.6 MPa and ductility of 29.75%.



Figure 6. ASTM E8 standard tensile samples (fracture sample)

4.3 Weldments impact test

Three standard V-notch Charpy test specimens prepared from dissimilar weldments according to ASTM E23 code to analyze weldments strength for different suitable applications. Cumulative V-notch Charpy test results for three specimen tests are 72 J for first specimens, 74 J for second specimen and 78 J for third specimen.

5. WELDMENTS SEM/EDS ANALYSIS

GTAW weldments employing filler wire ENiCrFe-3 SEM/EDS analysis represented in Figures 7, 8 and 9. The SEM of AISI 304 fusion line is found to have large sized voids as in Figure 7(a) and (b). The appearance in Monel 400 HAZ is very different, it's found to be non-spongy and more complex with the very small voids as in Figure 8(a), (b) and (c). The welding zone has texture base and adhesive sheets of weld metal observed clearly in Figure 9 with dendritic growth mode observed at weld zone. EDS analysis clearly shown Ni, Cu and Mn presence in high concentrations in Monel 400 HAZ. EDS analysis of AISI 304 HAZ shown Fe, Cr, Ni and Mn rich zone. Ni, Cr, Fe, Cu and C founded in weld zone with great amounts, Tables 3, 4 and 5 represent EDS analysis of Monel 400, AISI 304 and welding zone of dissimilar weldments.

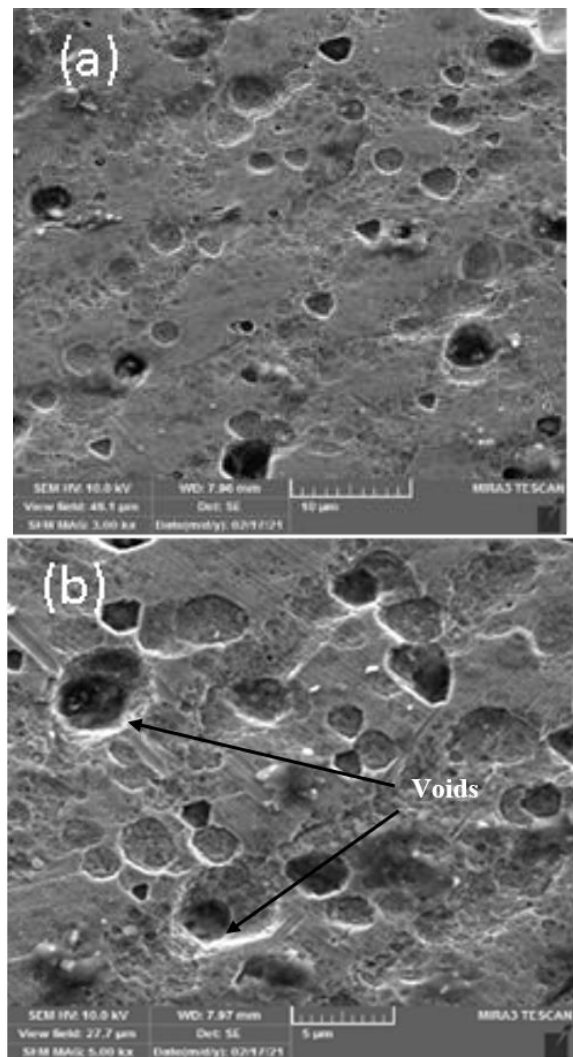


Figure 7. (a) and (b) SEM of AISI 304 PMZ

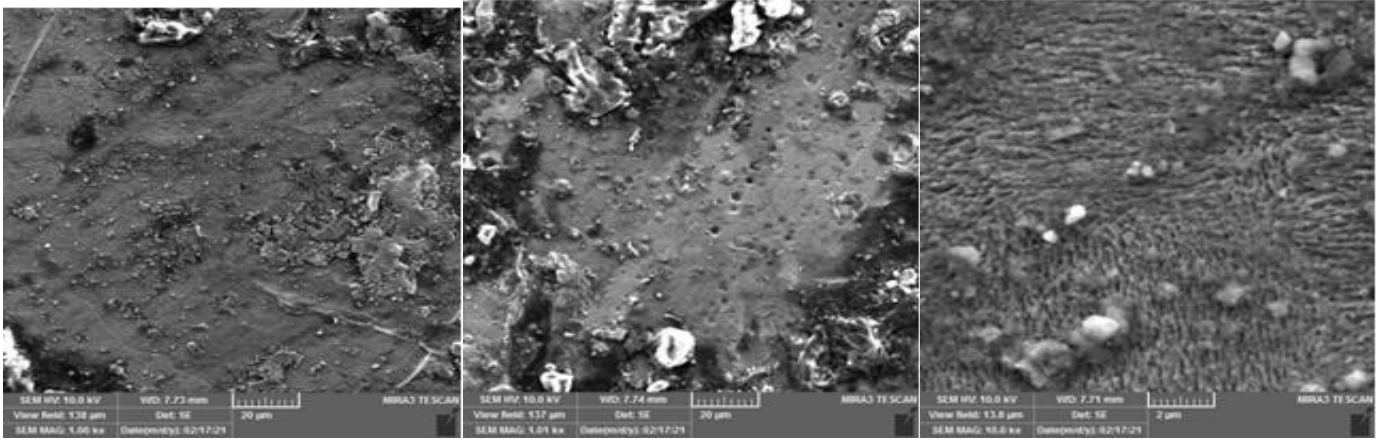


Figure 8. SEM of Monel 400 PMZ

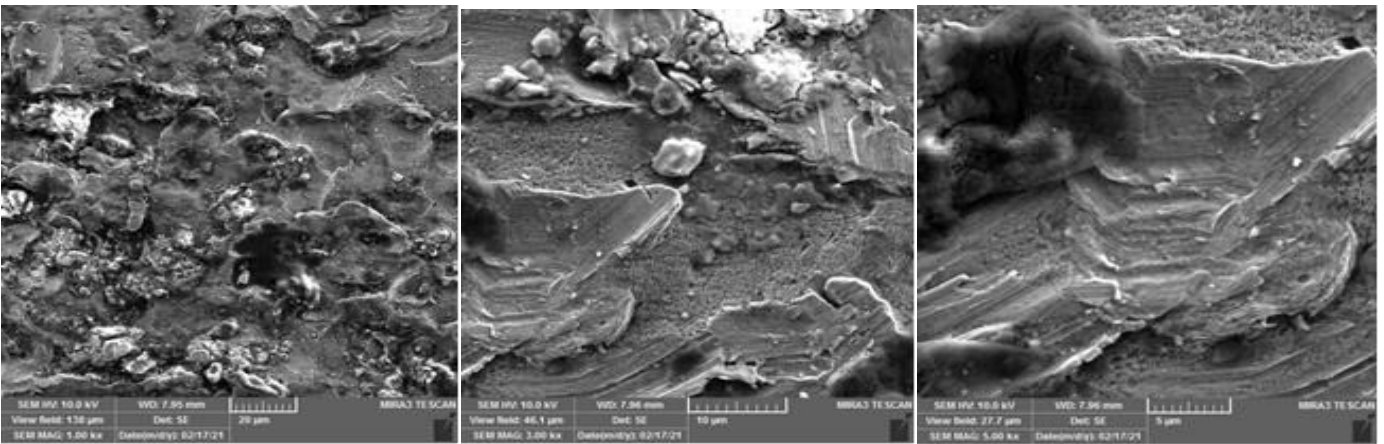


Figure 9. SEM of AISI 304 and Monel 400 welding zone

Table 3. Monel 400 GTAW weldments side EDS analysis

Elements Percentage (%)	Zone	
	HAZ	PMZ
Ni	63.54	59.25
Cu	32.52	27.41
C	0.32	0.32
Fe	2.21	9.82
Cr	Nil	24.10
Mn	1.07	4.16
O	0.17	0.45
Si	0.23	0.7
Al	Nil	0.4
Mo	Nil	0.57
Nb	Nil	1.3

Table 4. AISI 304 GTAW weldments side EDS analysis

Elements Percentage (%)	Zone	
	HAZ	Fusion line
Ni	8.9	31.70
Cu	Nil	Nil
C	1.35	0.08
Fe	65.13	45.70
Cr	21.60	14.01
Mn	1.91	1.47
O	Nil	0.73
Si	Nil	Nil
Al	Nil	0.14
Mo	1.45	3.84
Nb	Nil	2.33

Table 5. Monel 400 and AISI 304 GTAW welding zone EDS analysis

Elements Percentage (%)	Zone
	Welding Zone
Ni	65.3
Cu	4.64
C	0.14
Fe	9.90
Cr	17.52
Mn	0.95
O	Nil
Si	0.17
Al	Nil
Mo	0.24
Nb	1.14

6. DISCUSSION

6.1 Microstructure results discussion

Monel 400 HAZ microstructure in Figure 2(a), (b), (c) and (d) demonstrated coarse grains size at (HAZ) microstructure with Ni-Cu second phase formation, grains size coarsening can be observed in structure due to GTA welding heat. Also, partial melting zone (PMZ) formation can be easily observed in Monel HAZ and weld side of joint interface inside the HAZ. This zone formed when there is a zone of Monel parent metal heated just below liquid temperature but at the same time, above metal solid temperature, this means this zone only

partially melted and called partially melted zone (PMZ). Because of good thermal conductivity and low heat capacity of monel 400 alloy, relatively big, about 2 mm, PMZ zone created adjacent to welding fusion line. In PMZ most of interdendritic solidification mode which observed in welding zone just after fusion line and the grain boundaries fully melted and performed as channels to convey welding melt metal from welding pool to the root face, and creating PMZ melted and resolidified layers [17]. PMZ phenomenon is considerable for fusion welding technology, like GTAW, when the input heat is high to melting and joining the parts. Welding procedure for this reason is very critical to successfully joining Monel 400 with AISI 304 alloys to avert shrinkage porosity or holes in welding microstructure solidification in weld pool. Therefore, it's very important to understanding PMZ formation mechanism, And as a result understanding loss of ductility and hot cracking formation and phenomena in dissimilar welded joints [18]. Partially melted zone in Monel joint also formed low melting austenite eutectic carbide during solidification process and elements like Mn and Cr will be depleted from the welding zone toward monel interface side. Nickel reduction in PMZ weaker stabilization driving force of austenite on low temperatures during cooling, which when associated to high defunded carbon content from base metal consider a perfect condition for martensite creation, even with slower cooling rate conditions. However, due to high nickel concentration on PMZ of welds deposited when employed nickel alloys electrodes, austenite stabilizes on larger area inside PMZ, and because that only thin martensite layer expected to formed in welding zone deposited metal welded by these alloys.

AISI 304 HAZ side microstructure examination reveals changes in grain size, but no precipitation and sensitization evidences can be detected. Also, fine austenitic grains size noticed near fusion line and twinning randomly grain structure observed in little amount. Figure 3(a), (b), (c) and (d) shown formation of welding filler metal debilitation area or unmixed zone (UZ), intermediate mixed zone and hard zone often created in like these joints. The unmixed zone (UZ) had laminar layer microstructure and formation when small fractions of base metal completely melted and resolidified without undergo filler metal dilution. Unmixed zone (UZ) created when fusion zone has a thin completely melted and resolidified region adjacent to fusion line, where base metal quickly melted and solidified produced composition similar to parent metal known as unmixed or (chilled) zone [19], for example, when AISI 304 st.st welded using high chromium-nickel filler like ERNiFeCr-2, chromium and nickel concentration gradients founded in fusion zone, where unmixed zone has a structure with chemical composition similar to parent metal. No evidence of carbide precipitation was observed in AISI 304 HAZ and base metal from Figure 3(a), (b) and (c), but clearly grain growth observed due to the welding heat effects. UMZ formation causes in segregation during weld metal solidification and transformation of fractions from weld metal side which smaller than that in AISI 304 HAZ side, this process makes weld metal suffer dense segregation. In welding zone neighbor, the cooling rate in AISI 304 side is higher than fusion line and welding zone, resulting in longer exposure time to the sensitive temperature range for welding zone and fusion line. This exposure causes segregation of important elements like Mo and precipitations of other elements in weld zone side, a chromium-depleted zone may appear around these precipitations, which created

soft zone and activated surface to pitting corrosion, some pits can rapidly form in this zone and propagate in very fast rate, which deeply affected pitting corrosion resistance and weldment toughness. El-Aziz et al. [20] and Liou et al. [21] results found similar pitting corrosion holes from precipitations in welding process.

Welding zone microstructure in Figure 4(a), (b), (c) and (d) shows interdendritic solidification microstructure formation in weld region just near the fusion line, also the microstructure demonstrated clearly partial melting zone (PMZ) formation just after the fusion line. Interdendritic network consisting elements like Ni, Cr, Fe, Cu as in Figure 4(a), (b). The region far from the fusion line and welding zone center demonstrated clearly epitaxial solidification as in Figure 4(c) and (d), migrated grain boundaries also observed clearly at welding zone.

Since welding metal in Figure 4(c) and (d) illustrated existence of cellular solidification structure of welding zone contains some copper, secondary phases formation also can be observed; secondary phases formation makes welding metal more suspected for hot cracking defect. The globular precipitates and oxide inclusions distributed in welding zone matrix will affect joint properties. Formation of migrated grain boundaries (MGBs) can be observed clearly in Figure 4(c), (d) which most preferred austenitic welding metals. Weld metals with migrated grain boundaries (MGBs) as reported by other research papers, are more sensitive to the ductility dip cracking (DDC) issues which formed all over migrated grains boundaries.

Migrated grains boundaries existence in solidified weld metal structure produced welding zone with good strength and strain hardening capacity. The increasing of yield strength in welding zone attributed to the high stresses needed to innated slip transmission process. Dislocation reactions that operate at grain boundary affects both strength and deformation behavior. high strength and good mechanical properties obtained when interfaces act as dislocations movement obstacles, but no significant changes expected in welding zone mechanical properties when welding interface microstructure acts as a sink or its transparent to dislocations movements cross the structure grains boundaries. Obvious studies have reported that grains boundary migration is possible during reheating processes sequence, like what happen in welding procedures with multipass techniques, migrated grain boundaries formation phenomena strongly related to the element's diffusion and its effects in microstructure crystal lattices and crystal misorientation across grains boundaries and inclination of boundary plane [22], which effected by welding procedure heating cycle. Boundary migration initiated in welding zone solidified structure by bulges formation and expansion in boundary which grow into adjacent grains in another direction, spatial distribution and directions of these bulges occurred in random mode [22]. In this study, GTAW multipass procedure used to join these dissimilar metals, multipass procedure will normally produce high heat input value to the welding zone cause migration of grain boundaries phenomena. However microscopic and SEM images state that ductility dip cracking is not being recorded because of high amounts of Nb and Mo presence in unmixed zone (UZ) which formed adjacent to fusion line of AISI 304 when base metal melted and then quickly solidified, dynamic recrystallization classified as one of most important originators of DDC.

Dynamic recrystallization can define as a phenomenon that occurs when material strained in high temperatures range.

When that happen new grains formation in the high stress concentration locations like grains boundaries triple points, but the DDC agreed mechanism upon most researcher's state on that DDC is grains boundaries sliding phenomenon. Grains boundaries sliding generated stresses on grains boundaries triple points in weld metal microstructure [23], Nb and Mo had master effect in reduced weld metal DDC susceptibility because two reasons, the first one because Nb addition to weld metal structure formed NbC at solidification end. NbC formation pinned welding metal microstructure grains boundaries and tortuous the dislocations movements bath, also grains boundaries pinning created mechanical locking inhibited grain boundary sliding and therefore DDC.

The second reason related with Mo addition to welding zone microstructure, Mo addition forms M₂₃C₆ which precipitate in grains boundaries, carbide precipitate effects are uncertain whether helps with DDC mitigate, or it contributes to other effect. Noecker and DuPont [24] hypothesized effects of localized stress which forms at grains boundaries carbide interface and locking boundaries slipping.

Young et al. [25] proposed that (Fe,Cr)₂₃C₆ carbides formation is the major contributor in DDC initiation, because its generated localized solidification stresses during cooling. Nb or Ti additions forms MC carbides and reduce (Fe,Cr)₂₃C₆ formation and decreased welding microstructure DDC susceptibility, because DDC is precipitation cracking mechanism according to his work. This is not always true because austenitic alloys like AISI304 stainless steel can be susceptible to DDC even when no carbides precipitation occurred and unmixed zone microstructure with high chromium and nickel concentration and elements' gradients from fusion zone to UZ and HAZ in this research prove this fact.

6.2 SEM and EDS results discussion

SEM in Figure 7(a) and (b) of AISI 304 unmixed zone (UZ) is founded to have large sized voids disclose the fact of these weldments expected to failed with ductile mode fracture owing to micro and macro-voids existence, these large sized voids as discussed earlier in UZ formation mechanism could form from the segregation phenomena which cause very sensitive structure to pitting corrosion.

SEM in Figure 8 of PMZ in Monel side shown different uniform texture with no or few voids which increased welding metal mechanical properties. Welding zone SEM in Figure 9 has an austenitic texture with carbide, which is the favor of MGBs phenomena as reported by other studies [22]. EDS Analysis in Table 3 for Monel 400 HAZ and PMZ shows high nickel concentration on PMZ, this effects austenite stabilizes on larger area inside PMZ, and because that only thin martensite layer expected to formed in welding zone deposited metal. Also, chemical profile of PMZ on Monel interface which obtained from EDS analysis shows highlighting Fe, Cr and Ni percentages. From welding zone to PMZ planar region a gradual increasing in Ni and Cr content and reduction of Fe content can be observed. AISI 304 HAZ and PMZ EDS Analysis in Table 4 reflected the effects of unmixed zone UZ and soft zone formation EDS demonstrated the formation of soft and brittle zone in HAZ due the segregation of Mo from welding zone to fusion line and HAZ direction, and depleting of Cr toward welding zone direction which resulted in toughness and ductility leakage with reducing in pitting corrosion resistance in AISI 304 HAZ and fusion line.

Welding zone EDS shown high percentage of important elements like Ni, Cr, Fe and C which produced austenitic microstructure with MGB and carbide precipitation on grains boundary, this texture resulted in good mechanical properties to the welding zone compering with the neighbor zones.

6.3 Mechanical tests results discussion

Microhardness readings of weldments in Figure 5 showed that the welding zone recorded a maximum value compared to other zones of weldment. Presence of hard phases like NbC, (Nb, Mo) C formation evidence from SEM/EDS analysis and MGB formation in welding zone microstructure can be proofed clearly in microhardness profile values. highest hardness recording in welding zone because of metallic carbides presence which enhanced strength of weldments, AISI 304 unmixed zone and soft zone formation strongly involved in tensile test fracture location which marked in stainless steel side of weldments as show in Figure 6. As discussed, and explained in UZ formation in AISI 304 side, this zone will suffer from strong leakage in toughness and ductility with reduction in pitting corrosion resistance which forms voids in HAZ microstructure weaken this zone. V-notch Charpy test results certificated the microstructure and SEM results which reflected the highest toughness value of welding zone structure comparing with the other zones. Hardness test and V-notch Charpy test results well agreed with tensile test results and can certificated the SEM/EDS and microstructures results.

The most important features of the proposed method of this research are the ability to predicated welding zone and HAZ microstructure and mechanical properties connected to it by applying this study results which demonstrated that successful dissimilar joints of Monel 400 nickel alloy and 304 stainless steel can be produced by employing GTAW technology and ENiCrFe-2 welding filler. In another hand, the amount of input heat to welding zone is essential factor in dissimilar fusion welding and it's very difficult to precise control of welding heat in like this method which consider the main limitation of this study beside other limitations like the needed to professional TIG welder, which can be eliminated by automation welding process.

Development of this research in future work can be done by studying the impact of Mo and Ni nano particles addition to welding zone and study welding zone alteration according to that addition or changing welding current mode in TIG technology to pulse mode and control the time between current pulse to control the amounts of heat input.

7. CONCLUSIONS

(1) Monel 400 HAZ microstructure demonstrated coarse grains size with Ni-Cu second phase formation, grains size coarsening can be observed in structure due to GTA welding heat. Also, partial melting zone (PMZ) formation can be easily observed in Monel HAZ and weld side of joint interface inside the HAZ. Because of good thermal conductivity and low heat capacity of Monel 400 alloy, relatively big, about 2 mm, PMZ zone created adjacent to welding fusion line.

(2) AISI 304 HAZ side microstructure examination reveals changes in grain size, but no precipitation and sensitization evidences can be detected inside the HAZ. Also, fine austenitic grains size noticed near fusion line and twinning

randomly grain structure observed in little amount. Microstructure shown formation of welding filler metal debilitation area or unmixed zone (UZ), The unmixed zone (UZ) had laminar layer microstructure produce zone with leakage in toughness and ductility with low pitting corrosion resistance.

(3) Welding zone microstructure shows interdendritic solidification microstructure formation in weld region just near the fusion line, and clearly partial melting zone (PMZ) formation just after the fusion line. The region far from the fusion line and welding zone center demonstrated clearly epitaxial solidification, migrated grain boundaries (MGB) also observed clearly at welding zone. welding metal illustrated existence of cellular solidification structure; secondary phases formation also can be observed; secondary phases formation. The globular precipitates and oxide inclusions distributed in welding zone matrix will affect joint properties.

(4) Migrated grains boundaries existence in solidified weld metal structure produced welding zone with good strength and strain hardening capacity. The increasing of yield strength in welding zone attributed to the high stresses needed to innated slip transmission process. Dislocation reactions that operate at grain boundary affects both strength and deformation behavior. high strength and good mechanical properties obtained when interfaces act as dislocations movement obstacles.

(5) Alloying elements like Nb and Mo addition, promoted carbides formation tendency at solidification end and its very effective techniques to improving DDC resistance with nickel base filler.

(6) ENiCrFe-2 filler and GTAW technology can be used in dissimilar Monel 400 alloy and AISI 304 fusion welding. Weldments tensile test fracture happened in stainless steel HAZ side as direct effect of carbon and other important elements depletion. High hardness value in welding zone results from high concentration of carbon and carbide formation and formation of the second phases in fusion line and welding zone, welding zone had good toughness according to V notch test due to austenitic weld zone microstructure with (MGBs) phenomena.

REFERENCES

- [1] Davis, J.R. (2000). ASM Specialty Handbook: Nickel, Cobalt, and Their Alloys.
- [2] Lippold, J.C., Kotecki, D.J. (2005). Welding Metallurgy and Weldability of Stainless Steels. Wiley-Interscience.
- [3] Ramkumar, K.D., Arivazhagan, N., Narayanan, S., Karthikeyan, S. (2012). Hot Corrosion Behavior of Dissimilar GTA Welded Monel 400 and AISI 304. In: Ponnambalam, S.G., Parkkinen, J., Ramanathan, K.C. (eds) Trends in Intelligent Robotics, Automation, and Manufacturing. IRAM 2012. Communications in Computer and Information Science, vol 330. Springer, Berlin, Heidelberg. https://doi.org/10.1007/978-3-642-35197-6_50
- [4] Devendranath Ramkumar, K., Arivazhagan, N., Narayanan, S. (2012). Effect of filler materials on the performance of gas tungsten arc welded AISI 304 and Monel 400. *Materials & Design*, 40: 70-79. <https://doi.org/10.1016/j.matdes.2012.03.024>
- [5] Ghazi, A., Sabeeh, M., Salloum, A. (2022). Microstructure variation effects influence on characteristics and mechanical properties of Monel 400 and low alloy steel (ASTM 387-Gr.11) GTAW dissimilar joint. *Eastern-European Journal of Enterprise Technologies*, 5(12(119)): 13-20. <https://doi.org/10.15587/1729-4061.2022.266264>
- [6] Nallusamy, M., Suriyaprakash, M., Kiran, K. (2022). Experimental investigations on mechanical properties and microstructure of TIG welded monel 400 alloys. *Materials Today: Proceedings*, 62(Part 4): 2261-2265. <https://doi.org/10.1016/j.matpr.2022.03.502>
- [7] Yelamasetti, B., Kumar, S., Sridhar Babu, B., Vishu Vardhan, T., Gunda, V.R. (2019). Effect of filler wires on weld strength of dissimilar pulse GTA Monel 400 and AISI 304 weldments. *Materials Today: Proceedings*, 19(Part 2): 246-250. <https://doi.org/10.1016/j.matpr.2019.06.759>
- [8] Balram, Y., Sridhar Babu, B., Vishnu Vardhan, T., Venkat Ramana, G., Bhanu Prabhu Chakradhar, G. (2019). Residual stress analysis of dissimilar tungsten inert gas weldments of AISI 304 and Monel 400 by numerical simulation and experimentation. *Materials Today: Proceedings*, 19(Part 2): 478-483. <https://doi.org/10.1016/j.matpr.2019.07.639>
- [9] Mishra, D., Vignesh, M.K., Ganesh Raj, B., Srungavarapu, P., Devendranath Ramkumar, K., Arivazhagan, N., Narayanan, S. (2014). Mechanical characterization of Monel 400 and 316 stainless steel weldments. *Procedia Engineering*, 75: 24-28. <https://doi.org/10.1016/j.proeng.2013.11.005>
- [10] Devendranath Ramkumar, K., Arivazhagan, N., Narayanan, S. (2012). Effect of filler materials on the performance of Gas Tungsten arc welded AISI 304 and Monel 400. *Materials & Design*, 40: 70-79. <https://doi.org/10.1016/j.matdes.2012.03.024>
- [11] Arivazhagan, N., Singh, S., Prakash, S., Reddy, G.M. (2011). Investigation on AISI 304 austenitic stainless steel to AISI 4140 low alloy steel dissimilar joints by gas tungsten arc, electron beam and friction welding. *Materials & Design*, 32(5): 3036-3050. <https://doi.org/10.1016/j.matdes.2011.01.037>
- [12] Shah Hosseini, H., Shamanian, M., Kermanpur, A. (2011). Characterization of microstructures and mechanical properties of Inconel 617/310 stainless steel dissimilar welds. *Materials Characterization*, 62(4): 425-431. <https://doi.org/10.1016/j.matchar.2011.02.003>
- [13] Haddad-Sabzevar, M., Haerian, A., Seied-Hosseinzadeh, H. (2009). A stochastic model for austenite phase formation during arc welding of a low alloy steel. *Journal of Materials Processing Technology*, 209(8): 3798-3807. <https://doi.org/10.1016/j.jmatprotec.2008.08.039>
- [14] Naffakh, H., Shamanian, M., Ashrafizadeh, F. (2009). Dissimilar welding of AISI 310 austenitic stainless steel to nickel-based alloy Inconel 657. *Journal of Materials Processing Technology*, 209(7): 3628-3639. <https://doi.org/10.1016/j.jmatprotec.2008.08.019>
- [15] DuPont, J.N., Lippold, J.C., Kiser, S.D. (2009). Welding Metallurgy and Weldability of Nickel Base Alloys. John Wiley & Sons, Inc., Hoboken, New Jersey.
- [16] Alber Sadek, A., Abass, M., Zaghloul, B., Elrefaey, A., Ushio, M. (2000). Investigation of dissimilar Joints between Low Carbon steel and Monel 400. *Trans, JWRI*; 29(1): 21-28.
- [17] Kou, S. (1987). Welding Metallurgy. John Wiley and Sons.

- [18] Villars, P., Prince, A., Okamoto, H. (1990). Handbook of Ternary Alloy Phase Diagrams. American Society for Metals, Metals Park, p. 3933.
- [19] Soysal, T., Kou, S., Tat, D., Pasang, T. (2016). Macro segregation in dissimilar-metal fusion welding. *Acta Materialia*, 110: 149-160. <https://doi.org/10.1016/j.actamat.2016.03.004>
- [20] El-Aziz, A.M., El Meleigy, A.E., Benohanian, N.V., Exner, H. (2009). Corrosion behavior of laser and TIG welded austenitic stainless steel. *Egyptian Journal of Chemistry*, 83.
- [21] Inoue, H., Koseki, T. (2013). Solidification mechanism of austenitic stainless steel weld metals with primary ferrite solidification. In *Trends in Welding Research 2012: Proceedings of the 9th International Conference*, p. 242.
- [22] Winning, M., Gottstein, G., Shvindlerman, L.S. (2002). On the mechanisms of grain boundary migration. *Acta Materialia*, 50(2): 353-363. [https://doi.org/10.1016/S1359-6454\(01\)00343-3](https://doi.org/10.1016/S1359-6454(01)00343-3)
- [23] Fenske, J.A. (2010). Microstructure and hydrogen induced failure mechanisms in iron nickel weldments. Urbana: University of Illinois.
- [24] Noecker, I.I.F.F., DuPont, J.N. (2009). Metallurgical investigation into ductility dip cracking in Ni-based alloys: Part I. *Welding Journal*, 88(1): 7-s-20-s.
- [25] Ramirez, A.J., Lippold, J.C. (2004). High temperature cracking in nickel-base weld metal, Part 2: Insight into the mechanism. *Materials Science and Engineering: A*, 380(1-2): 245-258. <https://doi.org/10.1016/j.msea.2004.03.075>